Comparison of classical chaos with quantum chaos

2004 J. Phys. A: Math. Gen. 37 6251

(http://iopscience.iop.org/0305-4470/37/24/004)

INSTITUTE OF PHYSICS PUBLISHING JOURNAL OF PHYSICS A: MATHEMATICAL AND GENERAL

J. Phys. A: Math. Gen. **37** (2004) 6251–6265 PII: S0305-4470(04)75048-9

Comparison of classical chaos with quantum chaos

L A Caron[1], D Huard[1], H Kröger[1], G Melkonyan[1], K J M Moriarty[2] and L P Nadeau[1]

[1] Département de Physique, Université Laval, Québec, Québec G1K 7P4, Canada
[2] Department of Mathematics, Statistics and Computer Science, Dalhousie University, Halifax NS B3H 3J5, Canada

E-mail: hkroger@phy.ulaval.ca

Received 16 January 2004
Published 2 June 2004
Online at stacks.iop.org/JPhysA/37/6251
doi:10.1088/0305-4470/37/24/004

Abstract

We investigate chaotic behaviour in a 2D Hamiltonian system—oscillators with anharmonic coupling. We compare the classical system with the quantum system. Via the quantum action, we construct Poincaré sections and compute Lyapunov exponents for the quantum system. We find that the quantum system is globally less chaotic than the classical system. We also observe with increasing energy the distribution of Lyapunov exponents approaching a Gaussian with a strong correlation between its mean value and energy.

PACS numbers: 03.65.−w, 05.45.Mt

1. Introduction

Quantum chaos, which denotes properties of quantum systems whose underlying classical system is chaotic, has been experimentally observed in irregular energy spectra of nuclei, of atoms perturbed by strong electromagnetic fields [1]. In a weak exterior magnetic field, however, a hydrogen atom shows a level distribution being neither Poissonian nor Wignerian. How can we then compare classical chaos with quantum chaos? Is the quantum system more or less chaotic than the corresponding classical system? An understanding of how classically regular and chaotic phase space is reflected in quantum systems is an open problem, since semiclassical methods of quantization (EKB, Gutzwiller's trace formula) are not amenable to mixed dynamical systems [2]. In order to describe nearest neighbour energy level spacing distributions for mixed systems, workers have used different approaches. Percival [3] has suggested a distribution based on a division of phase space into regular and irregular regions. Brody [4] has suggested a phenomenological fit between a Wigner and a Poisson distribution. Izrailev [5] suggested a distribution based on the concept of quantum localization. Another interpolation between ensembles has been proposed by Lenz and Haake [6]. The interpolating

distribution proposed by Berry and Robnik [7] uses an interpolation parameter determined from classical phase space.

In order to address the above questions, workers have suggested concepts to reintroduce trajectories into quantum mechanics. One possibility is the use of the standard effective action, which takes into account quantum corrections of the classical action. Cametti *et al* [8] have considered the model of the 2D anharmonic oscillator and computed the effective action via loop ($\hbar$) expansion to low order. Another approach is Bohm's interpretation of quantum mechanics which expresses the Schrödinger equation in polar form. It allows us to introduce the concept of a particle trajectory and hence a quantum equivalent phase space. This approach has been used by Schwengelbeck and Faisal [9] to describe chaos in the kicked rotor and later by other workers for the 2D anisotropic harmonic oscillators [10], the hydrogen atom in an external electromagnetic field [11] and coupled anharmonic oscillators [12]. For the kicked rotor in 1D, which is classically chaotic, it turns out that the quantum system is nonchaotic, i.e. the quantum Kolmogorov–Sinai entropy goes to zero [9] (rediscovered in [12]). In contrast to that, the 2D anisotropic harmonic oscillator, being classically non-chaotic, has been reported to exhibit quantum chaos [10].

A comparison with respect to chaotic behaviour of the classical system and the quantum system has been investigated also in field theoretical models. Casetti *et al* [13] considered the large N limit of N-component ϕ^4 oscillators in the presence of an external field. Using mean field theory they observed a strong suppression of quantum chaos due to quantum corrections moving the system away from a hyperbolic fixed point responsible for classical chaos. Matinyan and Müller [14] considered the model of massless scalar electrodynamics, which is classically chaotic. Using effective field theory and loop expansion, they noticed that quantum corrections increase the threshold for chaos by modifying the ground state of the system.

To address the above questions, we apply the concept of the quantum action, developed in [15–20]. It expresses quantum transition amplitudes $G(x_{\rm fi}, t_{\rm fi}; x_{\rm in}, t_{\rm in})$ in terms of a local action—the quantum action—$\tilde{S}[x]$ defined by

$$\begin{aligned} G(\vec{x}_{\rm fi}, t = T; \vec{x}_{\rm in}, t = 0) &= \sum_{\text{trajectories}} \tilde{Z} \exp[\mathrm{i}\tilde{S}[\tilde{\vec{x}}_{\rm traj}]/\hbar] \\ \tilde{S}[\vec{x}] &= \int_0^T \mathrm{d}t\, \frac{1}{2}\tilde{m}\dot{\vec{x}}^2 - \tilde{V}(\vec{x}(t)) \qquad \tilde{\vec{x}}_{\rm traj} : \delta\tilde{S}[\tilde{\vec{x}}_{\rm traj}] = 0. \end{aligned} \tag{1}$$

Here $\tilde{S}$ is evaluated along its trajectory (stationary point of $\tilde{S}$) going from boundary point $(\vec{x}_{\rm in}, t = 0)$ to $(\vec{x}_{\rm fi}, t = T)$. There may be several such stationary points. The quantum action has been explored numerically [15–17, 20] for confinement-type potentials (bound state spectrum), e.g. the inverse square potential and polynomial potentials. The numerical studies taking into account only one trajectory (of lowest action) show that the parameters of the quantum action vary smoothly with transition time T, interpolating between the classical action at $T = 0$ and some 'deep' quantum action in the asymptotic regime $T \to \infty$. In the limit of large imaginary transition time, the quantum action has been proved to exist, and to give an exact parametrization of transition amplitudes [18]. Also in this limit analytical relations exist between the classical potential, the quantum potential and wavefunctions [19].

What is the physical interpretation of the quantum action and its trajectories? In the path integral representation of the transition amplitude occurs the classical action and all kinds of paths (zig-zag curves). In the quantum action representation occurs the quantum action but only some trajectories (differentiable curves). Thus we interpret the quantum action as a renormalization effect on the classical action. Quantum fluctuations appear as tuned parameters in the new action. This situation is similar to renormalization in solid state

physics: a charged particle propagating in the solid interacts with atoms. This results in an effective mass and charge, different from that of free propagation.

The local quantum action and its trajectories allow us to construct a quantum analogue phase space. From that one can compute quantum Poincaré sections, Lyapunov exponents or the Kolmogorov–Sinai entropy like in classical nonlinear dynamics. This gives a new vista on quantum chaos. First results of a numerical study have been reported in [17]. The quantum action has been found useful also to characterize quantum instantons [16]. The definition of the quantum action looks conspicously similar to that of Bohm's parametrization of the wavefunction. So what is the difference and what is new here compared to previous studies of quantum chaos based on Bohm's approach? First, Bohm's approach considers the quantum system in a state given by a particular wavefunction. Hence the fluid dynamical motion depends on such wavefunction (via Bohm's quantum potential). The quantum action, however, is the same for all initial and final states of the transition amplitude, and depends only on transition time. Of course, the trajectories of the quantum action depend on initial and final boundary conditions. Second, in Bohm's approach, the mass of the particle occurring in the fluid dynamics picture is the same as in the original Hamiltonian. In the quantum action, the mass is renormalized and in general differs in value from the classical mass. Finally, in contrast to Bohm's approach, the quantum action is very close in functional form to the classical action, and hence allows a direct and detailed comparison of phase space, as will be shown below.

2. Existence and analytical form of quantum action in the limit of large imaginary time

The proof of the existence of the quantum action in the limit of large imaginary time for Hamiltonian systems has been given for 1D in [18]. Because we consider in this work a 2D Hamiltonian system, and for sake of self-consistency we will outline the proof here for arbitrary dimension (in particular $D = 2, 3$). Moreover, we present nonlinear differential equations relating the classical potential to the quantum potential. Also the relation between the quantum action and supersymmetric quantum mechanics will be discussed. Let us go over to imaginary time $t \to -\mathrm{i}t$. Then the transition amplitude becomes the Euclidean transition amplitude

$$G_E(\vec{x}_{\mathrm{fi}}, T; \vec{x}_{\mathrm{in}}, 0) = \langle \vec{x}_{\mathrm{fi}} | \, \mathrm{e}^{-HT/\hbar} | \vec{x}_{\mathrm{in}} \rangle = \int [\mathrm{d}x] \exp\left[-\frac{1}{\hbar} S_E[\vec{x}] \right] \Bigg|_{\vec{x}_{\mathrm{in}}, o}^{\vec{x}_{\mathrm{fi}}, T} \tag{2}$$

the classical action becomes the Euclidean classical action

$$S_E[\vec{x}] = \int_0^T \mathrm{d}t \left\{ \frac{1}{2} m \dot{\vec{x}}^2 + V(\vec{x}) \right\} \tag{3}$$

and the quantum action becomes the Euclidean quantum action

$$\tilde{S}_E[\vec{x}] = \int_0^T \mathrm{d}t \left\{ \frac{1}{2} \tilde{m} \dot{\vec{x}}^2 + \tilde{V}(\vec{x}) \right\}. \tag{4}$$

Our goal is to prove for $T \to \infty$ that the Euclidean transition amplitudes can be expressed in terms of the Euclidean quantum action, using a single trajectory

$$\begin{aligned} G_E(\vec{x}_{\mathrm{fi}}, T; \vec{x}_{\mathrm{in}}, 0) &= \tilde{Z}_E \exp\left[-\frac{1}{\hbar} \, \tilde{\Sigma}_E \Big|_{\vec{x}_{\mathrm{in}}, 0}^{\vec{x}_{\mathrm{fi}}, T} \right] \\ \tilde{\Sigma}_E \Big|_{\vec{x}_{\mathrm{in}}, 0}^{\vec{x}_{\mathrm{fi}}, T} &= \tilde{S}_E[\tilde{\vec{x}}_{\mathrm{traj}}] \Big|_{\vec{x}_{\mathrm{in}}, 0}^{\vec{x}_{\mathrm{fi}}, T} = \int_0^T \mathrm{d}t \left\{ \frac{1}{2} \tilde{m} \dot{\tilde{\vec{x}}}_{\mathrm{traj}}^2 + \tilde{V}(\tilde{\vec{x}}_{\mathrm{traj}}) \right\} \Bigg|_{\vec{x}_{\mathrm{in}}}^{\vec{x}_{\mathrm{fi}}}. \end{aligned} \tag{5}$$

2.1. Necessary and sufficient conditions for the existence of the quantum action

For simplicity of notation we drop the subscript Euclidean. Let us make some assumptions on the potential $V(\vec{x})$: let $V(\vec{x}) \geqslant 0$. Let $V(\vec{x})$ be a smooth (sufficiently differentiable) function of $\vec{x}$ and let $V(\vec{x}) \to \infty$ when $|\vec{x}| \to \infty$. Moreover, let $V(\vec{x})$ have a single minimum. Also we assume that the ground state is non-degenerate. Because the Euclidean transition amplitude is given by a (Wiener) path integral with a positive Euclidean action, $G(\vec{y}, T; \vec{x}, 0) \geqslant 0$ for all $\vec{x}, \vec{y}$. Hence we can introduce a real function η such that

$$G(\vec{y}, T; \vec{x}, 0) = G_0 \exp[-\eta(\vec{y}, \vec{x})] \tag{6}$$

where G_0 is some constant (for fixed T) which takes care of the fact that G has a dimension $(1/L^D)$.

Comparing the parametrization of G in terms of the function η, equation (6), with its parametrization in terms of the quantum action, equation (5), this looks similar. In order to prove it we need to establish that $\eta(\vec{y}, \vec{x})$ can be expressed in terms of a local action $\tilde{S}$ evaluated along its trajectory $\tilde{\vec{x}}_{\text{traj}}$, such that

$$\eta(\vec{y}, \vec{x}) = \frac{1}{\hbar} \tilde{S}[\tilde{\vec{x}}_{\text{traj}}] \Big|_{\vec{x}, t=0}^{\vec{y}, t=T} \qquad \text{and} \qquad G_0 = \tilde{Z}. \tag{7}$$

This is a necessary and sufficient condition for the existence of the quantum action. In order to establish that those equations hold, we proceed in the following by establishing a number of equations equivalent to equation (7). At the end, we show that the last of those conditions can be satisfied.

First, we compute partial derivatives of η and Σ. Consider the functional derivative up to first order of the action $\tilde{S}$ around the stationary point, admitting also variation of boundary points, denoted by

$$\begin{aligned} &\tilde{\vec{x}}(t) = \tilde{\vec{x}}_{\text{traj}}(t) + \tilde{\vec{h}}(t) \qquad && \tilde{\vec{x}}_{\text{traj}}(t=0) = \vec{a} \qquad && \tilde{\vec{x}}_{\text{traj}}(t=T) = \vec{b} \\ &\tilde{\vec{h}}(t=0) = \delta\vec{a} && \tilde{\vec{h}}(t=T) = \delta\vec{b}. \end{aligned} \tag{8}$$

We obtain

$$\delta\tilde{S}[\tilde{\vec{x}}] = \tilde{\vec{p}}_{\text{traj}}(T) \cdot \delta\vec{b} - \tilde{\vec{p}}_{\text{traj}}(0) \cdot \delta\vec{a} + O(\tilde{h}^2). \tag{9}$$

On the other hand, one has

$$\delta\eta(\vec{b}, \vec{a}) = \vec{\nabla}_{\vec{y}} \eta(\vec{y}, \vec{a})|_{\vec{y}=\vec{b}} \cdot \delta\vec{b} + \vec{\nabla}_{\vec{x}} \eta(\vec{b}, \vec{x})|_{\vec{x}=\vec{a}} \cdot \delta\vec{a}. \tag{10}$$

Comparing equations (9), (10) for terms linear in $\delta\vec{a}$ and $\delta\vec{b}$, respectively, we find the following necessary and sufficient conditions for the existence of the quantum action,

$$\left\{ \begin{array}{l} -\frac{1}{\hbar}\tilde{\vec{p}}_{\text{traj}}(0) = \vec{\nabla}_{\vec{x}} \frac{1}{\hbar} \tilde{\Sigma}|_{\vec{x}}^{\vec{y}} = \vec{\nabla}_{\vec{x}} \eta(\vec{y}, \vec{x}) \\ \frac{1}{\hbar}\tilde{\vec{p}}_{\text{traj}}(T) = \vec{\nabla}_{\vec{y}} \frac{1}{\hbar} \tilde{\Sigma}|_{\vec{x}}^{\vec{y}} = \vec{\nabla}_{\vec{y}} \eta(\vec{y}, \vec{x}) \end{array} \right\} \quad \text{for all boundary points } (\vec{y}, \vec{x}). \tag{11}$$

Equation (11) is equivalent to

$$\frac{1}{\hbar} \tilde{\Sigma}|_{\vec{x}}^{\vec{y}} = \eta(\vec{y}, \vec{x}) \quad \text{modulo a global constant.} \tag{12}$$

The global constant can be absorbed into the constants G_0 and $\tilde{Z}$, respectively, and hence equation (11) is equivalent to equation (7).

2.2. Use of energy conservation

It remains to be shown how condition (11) can be satisfied. We do this by employing the principle of conservation of energy. The action given by equation (4) describes a conservative system, i.e., the force is derived from a potential and energy is conserved. In imaginary time, energy conservation reads

$$-\tilde{T}_{\rm kin} + \tilde{V} = \epsilon = \text{const} \tag{13}$$

which implies

$$\tilde{V}(\vec{b}) - \tilde{V}(\vec{a}) = \frac{1}{2\tilde{m}}\big(\tilde{\vec{p}}^{\,\rm fi}_{\rm traj}\big)^2 - \frac{1}{2\tilde{m}}\big(\tilde{\vec{p}}^{\,\rm in}_{\rm traj}\big)^2. \tag{14}$$

Thus combining equations (11) and (14), we find another necessary and sufficient condition for the existance of the quantum action: the quantum action exists and is local, if there is a mass $\tilde{m}$ and a local potential $\tilde{V}(\vec{x})$, such that

$$\frac{2\tilde{m}}{\hbar^2}[\tilde{V}(\vec{b}) - \tilde{V}(\vec{a})] = (\vec{\nabla}_{\vec{y}}\eta(\vec{y},\vec{a})|_{\vec{y}=\vec{b}})^2 - (\vec{\nabla}_{\vec{x}}\eta(\vec{b},\vec{x})|_{\vec{x}=\vec{a}})^2 \quad \text{holds for all } \vec{a},\vec{b}. \tag{15}$$

2.3. Feynman–Kac limit

Finally, we want to show that equation (15) can be satisfied in the limit $T \to \infty$. In this limit holds the Feynman–Kac formula

$$G(\vec{y},T;\vec{x},0) \underset{T\to\infty}{\longrightarrow} \langle\vec{y}|\psi_{\rm gr}\rangle\, {\rm e}^{-E_{\rm gr}T/\hbar}\langle\psi_{\rm gr}|\vec{x}\rangle \tag{16}$$

where $\psi_{\rm gr}$ is the ground state wavefunction and $E_{\rm gr}$ is the ground state energy. Here we use the assumption that the ground state is not degenerate. Equation (6) implies

$$G_0\, {\rm e}^{-\eta(\vec{y},\vec{x})} \underset{T\to\infty}{\longrightarrow} \langle\vec{y}|\psi_{\rm gr}\rangle\, {\rm e}^{-E_{\rm gr}T/\hbar}\langle\psi_{\rm gr}|\vec{x}\rangle. \tag{17}$$

From this we compute

$$\vec{\nabla}_{\vec{y}}\eta(\vec{y},\vec{x})|_{\vec{y}=\vec{b},\vec{x}=\vec{a}} \underset{T\to\infty}{\longrightarrow} = -\frac{\vec{\nabla}\psi_{\rm gr}(\vec{b})}{\psi_{\rm gr}(\vec{b})} \qquad \vec{\nabla}_{\vec{x}}\eta(\vec{y},\vec{x})_{\vec{y}=\vec{b},\vec{x}=\vec{a}} \underset{T\to\infty}{\longrightarrow} -\frac{\vec{\nabla}\psi_{\rm gr}(\vec{a})}{\psi_{\rm gr}(\vec{a})}. \tag{18}$$

Then the general condition (15) becomes

$$\frac{2\tilde{m}}{\hbar^2}[\tilde{V}(\vec{b}) - \tilde{V}(\vec{a})] \underset{T\to\infty}{\longrightarrow} \left(\frac{\vec{\nabla}\psi_{\rm gr}(\vec{b})}{\psi_{\rm gr}(\vec{b})}\right)^2 - \left(\frac{\vec{\nabla}\psi_{\rm gr}(\vec{a})}{\psi_{\rm gr}(\vec{a})}\right)^2 \quad \text{for all } \vec{a},\vec{b}. \tag{19}$$

This holds if we can find $\tilde{m}$ and $\tilde{V}(\vec{x})$, such that

$$\frac{2\tilde{m}}{\hbar^2}(\tilde{V}(\vec{x}) - \tilde{V}_0) = \left(\frac{\vec{\nabla}\psi_{\rm gr}(\vec{x})}{\psi_{\rm gr}(\vec{x})}\right)^2 \quad \text{for all } \vec{x} \tag{20}$$

where $\tilde{V}_0$ denotes the minimum of the potential. This condition can be satisfied. This establishes the existence of a local quantum action and finishes the proof.

2.4. Relation between classical and quantum potential

We continue to work in the limit $T \to \infty$. Let us consider the stationary Schrödinger equation for the ground state, which can be written in the form

$$\frac{\Delta\psi_{\rm gr}(\vec{x})}{\psi_{\rm gr}(\vec{x})} = \frac{2m}{\hbar^2}[V(\vec{x}) - E_{\rm gr}] \tag{21}$$

where m is the classical mass and V is the classical potential. Because the transition amplitude is positive, also the ground state wavefunction obeys $\psi_{\rm gr}(\vec{x}) \geqslant 0$ for all $\vec{x}$. Hence we can define the function $U(\vec{x})$,

$$U(\vec{x}) = \log \psi_{\rm gr}(\vec{x}). \tag{22}$$

Using equations (20), (21) we compute

$$\Delta U(\vec{x}) = \frac{2\tilde{m}}{\hbar^2}[\tilde{V}(\vec{x}) - \tilde{V}_0] + \frac{2m}{\hbar^2}[V(\vec{x}) - E_{\rm gr}]. \tag{23}$$

It can be cast in the form

$$\Delta U(\vec{x}) + (\vec{\nabla} U(\vec{x}))^2 = \frac{2m}{\hbar^2}[V(\vec{x}) - E_{\rm gr}] \qquad \frac{2\tilde{m}}{\hbar^2}[\tilde{V}(\vec{x}) - \tilde{V}_0] = (\vec{\nabla} U)^2. \tag{24}$$

The first equation is a generalized Riccati-type differential equation for the function $U(\vec{x})$. From its solution one can obtain the quantum potential, more precisely $\tilde{m}\tilde{V}(\vec{x})$. Hence, equations (24) constitute a transformation rule

$$mV(\vec{x}) \to \tilde{m}\tilde{V}(\vec{x}). \tag{25}$$

From the point of view of numerical solution, it may be advantageous to cast equation (24) in a slightly different form. Let us define

$$\vec{W}(\vec{x}) = \vec{\nabla} U(\vec{x}). \tag{26}$$

Then the generalized Riccati differential equation becomes

$$\vec{\nabla} \cdot \vec{W}(\vec{x}) + (\vec{W}(\vec{x}))^2 = \frac{2m}{\hbar^2}[V(\vec{x}) - E_{\rm gr}] \qquad \frac{2\tilde{m}}{\hbar^2}[\tilde{V}(\vec{x}) - \tilde{V}_0] = (\vec{W}(\vec{x}))^2. \tag{27}$$

2.5. Relation between quantum action and potentials in supersymmetric quantum mechanics

Starting with Witten's work [21] it was recognized that supersymmetry can be applied to quantum mechanics. In [22] the correspondence between the 1D Fokker–Planck equation with a bi-stable potential and supersymmetric quantum mechanics has been shown to facilitate the calculation of a small eigenvalue that controls the rate at which equilibrium is approached. Kumar *et al* [23] used the supersymmetric approach to compute the tunnelling exchange integral $t = E_1 - E_0$ and pointed out the Riccati differential equation between the classical and supersymmetric partner potential. Let us consider a 1D Hamiltonian system, which in the notation of [24] and using $\hbar = 2m = 1$ is given by

$$H_- = -\frac{{\rm d}^2}{{\rm d}x^2} + V_-(x) \tag{28}$$

where V_- denotes the standard classical potential. One can construct a supersymmetric partner potential $V_+(x)$,

$$V_+(x) = V_-(x) - 2\frac{\rm d}{{\rm d}x}\frac{\psi'_{\rm gr}}{\psi_{\rm gr}} = -V_-(x) + 2\left(\frac{\psi'_{\rm gr}}{\psi_{\rm gr}}\right)^2. \tag{29}$$

Defining a superpotential $W_s(x)$ by

$$W_s(x) = -\frac{\psi'_{\rm gr}}{\psi_{\rm gr}} \tag{30}$$

one obtains

$$V_\pm(x) = W_s^2(x) \pm \frac{{\rm d}W_s}{{\rm d}x} \tag{31}$$

Table 1. Parameters of classical action versus quantum action. $v_{22} = 0.25$, $T = 4.5$.

Parameter	Classical action	Quantum action
m	1	0.976(8)
v_0	0	1.3992(4)
v_2	0.5	0.5684(3)
v_{22}	0.25	0.2469(4)
v_4	0	−0.00067(7)

which is a Riccati-type equation. The following similarities are apparent. Comparing equations (26), (30) one finds

$$W(x) = -W_s(x) \tag{32}$$

which satisfy the corresponding Riccati differential equations (27), (31). The following remarks are in order. In the super-symmetric approach the mass is identical to the classical mass, while in the quantum action, the mass gets tuned, in general. In contrast to the super-symmetric quantum Hamiltonian, the quantum action gives a parametrization of quantum transition amplitudes (see equation (1)), which requires a tuning of the mass.

3. Model and its quantum action

In order to study full chaos the so-called K-system (2D Hamiltonian, potential $V = x^2y^2$) is widely used. It is almost globally chaotic, having small islands of stability [25]. In order to study mixed dynamics (entangling chaos and regular islands) it is numerically convenient to consider the following classical system [26]:

$$S = \int_0^T \mathrm{d}t\, \frac{1}{2}m(\dot{x}^2 + \dot{y}^2) - V(x, y) \qquad V = v_2(x^2 + y^2) + v_{22}x^2y^2. \tag{33}$$

The parameters of the classical action are given in table 1. The ground state wavefunction of the quantum system, obtained by solving the Schrödinger equation, is depicted in figure 1. The quantum action (see equation (1)) takes the form

$$\tilde{S} = \int_0^T \mathrm{d}t\, \frac{1}{2}\tilde{m}(\dot{x}^2 + \dot{y}^2) - \tilde{V}(x, y). \tag{34}$$

We need to determine the quantum mass (tuned mass) $\tilde{m}$ and the quantum potential $\tilde{V}(x, y)$. For large imaginary time T we have analytical results on the form of $\tilde{V}$. The function $\tilde{m}(\tilde{V}(x, y) - \tilde{V}_{\min})$ is given by equation (20) or equivalently by the solution of equation (27). This is depicted in figure 2. We need to determine $\tilde{m}$ and $\tilde{V}$ separately and also the parameter $\tilde{Z}$ of the quantum action. These have been computed numerically in a non-perturbative way from a global fit to transition amplitudes in imaginary time. For this purpose we made a polynomial ansatz for the quantum action of the following form:

$$\begin{aligned}\tilde{V}(x, y) = {} & \tilde{v}_0 + \tilde{v}_{11}xy + \tilde{v}_2(x^2 + y^2) + \tilde{v}_{22}x^2y^2 + \tilde{v}_{13}(xy^3 + x^3y) \\ & + \tilde{v}_4(x^4 + y^4) + \tilde{v}_{24}(x^2y^4 + x^4y^2) + \tilde{v}_{44}x^4y^4.\end{aligned} \tag{35}$$

We have computed transition amplitudes $G(\vec{x}_{\mathrm{fi}}, t_{\mathrm{fi}}; \vec{x}_{\mathrm{in}}, t_{\mathrm{in}})$ by solving the Schrödinger equation in imaginary time keeping the transition time T fixed. The determination of unknown parameters of the quantum action, such as $\tilde{Z}$, $\tilde{m}$, etc, requires as many equations as unknowns. In practice we use many equations (overdetermined system), by considering a large set of pairs of initial and final boundary points $(\vec{x}_j, \vec{x}_i)$ and the corresponding transition amplitudes. Next we make an initial guess for the unknown parameters, say $\tilde{Z}^{(0)}$, $\tilde{m}^{(0)}$, etc and solve the

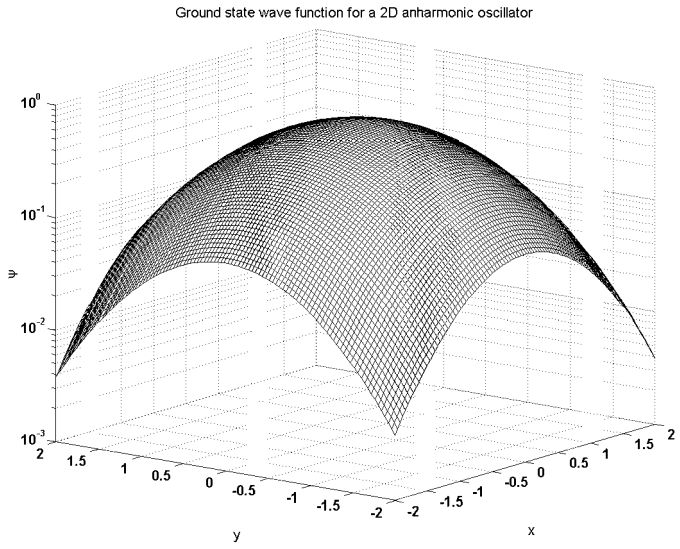

Figure 1. Ground state wavefunction $\psi_{\rm gr}(x, y)$.

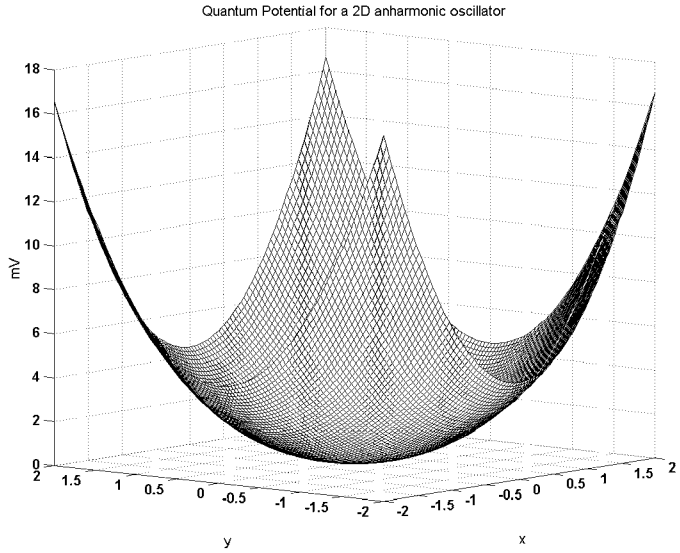

Figure 2. Quantum potential $\tilde{m}(\tilde{V}(x, y) - \tilde{V}_{\rm min})$.

Euler–Lagrange equations of motion derived from the quantum action $\tilde{S}^{(0)}$, for each pair of boundary points. Then we compute the error

$$\epsilon = \sum_{i,j=1}^{N} \left| G(\vec{x}_i, T; \vec{x}_j, 0) - \tilde{Z}^{(0)} \exp\left[\frac{\rm i}{\hbar}\, \tilde{S}^{(0)}\left[\tilde{\vec{x}}^{(0)}_{\rm traj}\right]\Big|_{\vec{x}_j,0}^{\vec{x}_i,T} \right] \right|^2 . \tag{36}$$

In order to eventually find the physical values of the unknown parameters we apply a variational principle, i.e. we search in the multi-parameter space to minimize the error globally (over all pairs of boundary points). For more details see [15]. As a result, the terms $\tilde{v}_{11}$, $\tilde{v}_{13}$, $\tilde{v}_4$, $\tilde{v}_{24}$, $\tilde{v}_{44}$

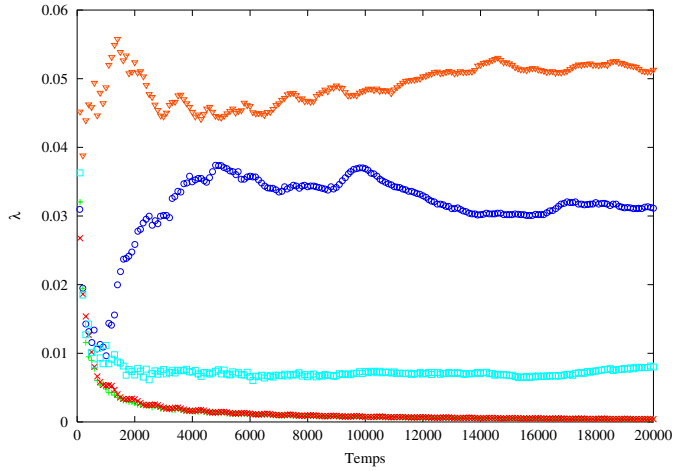

Figure 3. Typical time evolution of Lyapunov exponents. $v_{22} = 0.25$. $E = 2$.
(This figure is in colour only in the electronic version)

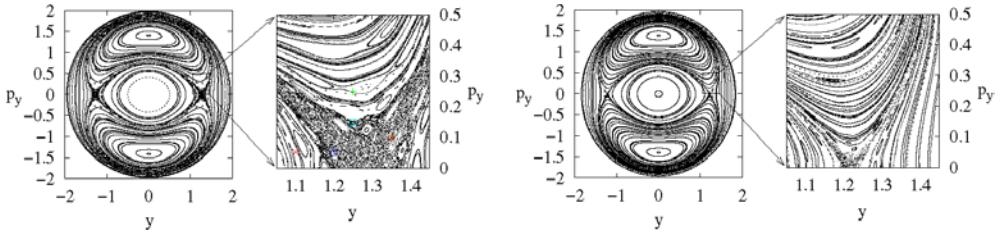

Figure 4. Poincaré section of the classical system (left) and the quantum system (right). $v_{22} = 0.25$. $E = 2$.

were found to be quite small or compatible with zero. The parameters of the corresponding quantum action for transition time $T = 4.5$ (large compared to dynamical time scale $T_{sc} = 1/E_{gr}$) and parameter $v_{22} = 0.25$ (which controls chaos) are shown in table 1. The parentheses give the estimated error of the fit. The numerical results presented below refer to $v_{22} = 0.25$ and $v_{22} = 0.05$. Before we present our comparison of classical chaos with quantum chaos, we ask what behaviour do we expect? In the 1D quartic potential quantum effects produce a strong positive quadratic term in the quantum action [15]. In the 1D double well potential, the quantum potential becomes softened, i.e., it has a lower barrier and closer minima. As a consequence, the instanton solutions of the quantum action are softer than the corresponding classical instantons [16]. Are such softening effects also occurring in chaotic phenomena?

4. Classical chaos versus quantum chaos

The notion of chaotic versus regular phase space is based on Lyapunov exponents ($\lambda > 0$ versus $\lambda \leqslant 0$). Numerically it is difficult to distinguish a small positive from a zero Lyapunov exponent. In order to discriminate those cases we followed the time evolution for a long time. We used $T_c = 20\,000$ to measure λ. This is depicted in figure 3. A comparison of Poincaré sections of the classical and the quantum system is shown in figure 4 for $v_{22} = 0.25$ and

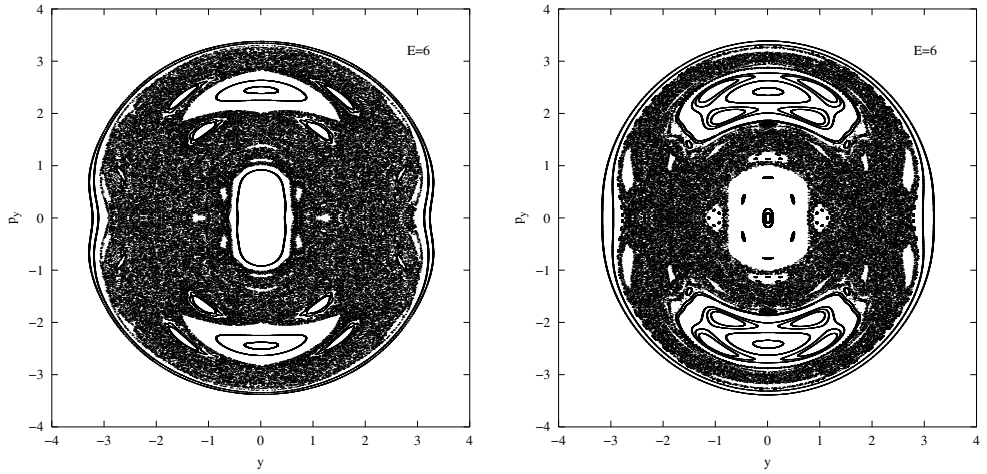

Figure 5. Poincaré section of the classical system (left) and the quantum system (right). $v_{22} = 0.25$. $E = 6$.

$E = 2$. One observes a smaller number of chaotic trajectories in the quantum case than in the classical case. In particular, this is visible near the hyperbolic fixed points (see the inset). The same comparison for some higher energy ($E = 6$) is shown in figure 5. With increasing energy the difference between classical and quantum phase space becomes more pronounced. In order to get a quantitative measure for chaotic versus regular phase space, we have chosen randomly a large number of initial conditions and computed the finite time Lyapunov exponent for each such trajectory. The distribution of these Lyapunov exponents in the neighbourhood of $\lambda = 0$ is shown in figure 6, and those for $0 < \lambda < 0.25$ is shown in figure 7. Figure 6 shows the distribution of Lyapunov exponents for different energies for the classical and quantum system. While $\lambda = 0$ corresponds to regular behaviour, $\lambda > 0$ indicates chaotic behaviour. For the purpose of numerically distinguishing the two regimes, we used this distribution to define some cut-off λ_c (vertical dashed line in figure 6). Figure 6 also shows the cumulative distribution $P(\lambda)$ (full line), which is a measure of the degree of regularity. As can be seen this curve is higher for the quantum system compared to the classical system. Moreover, figure 6 displays the coefficient R which denotes the ratio of chaotic phase space to total phase space. The distribution of positive Lyapunov exponents is displayed in figure 7. First, one observes a pronounced peak near zero, which has been magnified in figure 6. Second, with the increase of energy, the system becomes more chaotic, i.e. R increases. Third, with increasing energy, the distribution of positive Lyapunov exponents seems to approach a Gaussian shape.

Fourth, the width of the Gaussian (variance) diminishes with increasing energy. Fifth, with increasing energy, a strong linear correlation develops between the expectation value of λ and energy E, which can be represented by a linear fit $\langle\lambda\rangle = \lambda^{(0)} + \epsilon E$ (fit parameters are $\lambda^{(0)}_{\rm cl} = -0.040, \epsilon_{\rm cl} = 0.033$ and $\lambda^{(0)}_{\rm qm} = -0.026, \epsilon_{\rm qm} = 0.024$, i.e. $\epsilon_{\rm qm} < \epsilon_{\rm cl}$). All these features hold for both the classical system and the quantum system. A quantitative difference between classical and quantum system is apparent in the degree of chaoticity R, shown in figures 6 and 7. The corresponding results for $v_{22} = 0.05$ are given in figures 8 and 9, which show qualitatively the same behaviour. The basic difference between the data for $v_{22} = 0.25$ and $v_{22} = 0.05$ shows up in the degree of chaoticity R which is smaller for the latter, and also in the location of the peak in the distribution of positive Lyapunov exponents (compare figures 7 and 9), which is also smaller for the latter. This shows that the parameter v_{22}, which controls

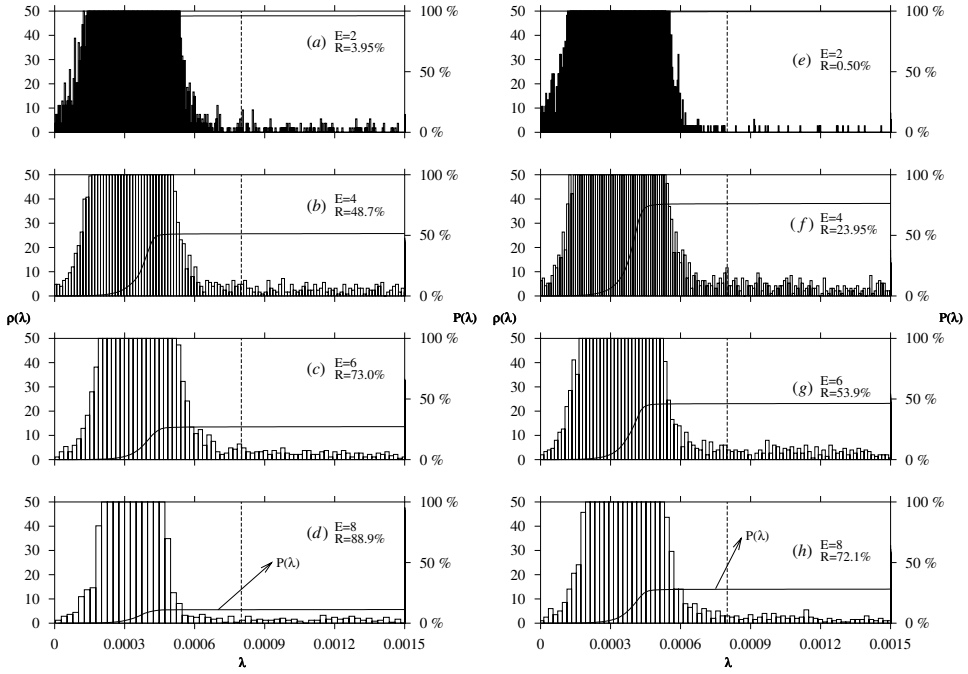

Figure 6. Distribution of Lyapunov exponents near $\lambda = 0$ for different energies E. Classical system (left column) and quantum system (right column). $v_{22} = 0.25$.

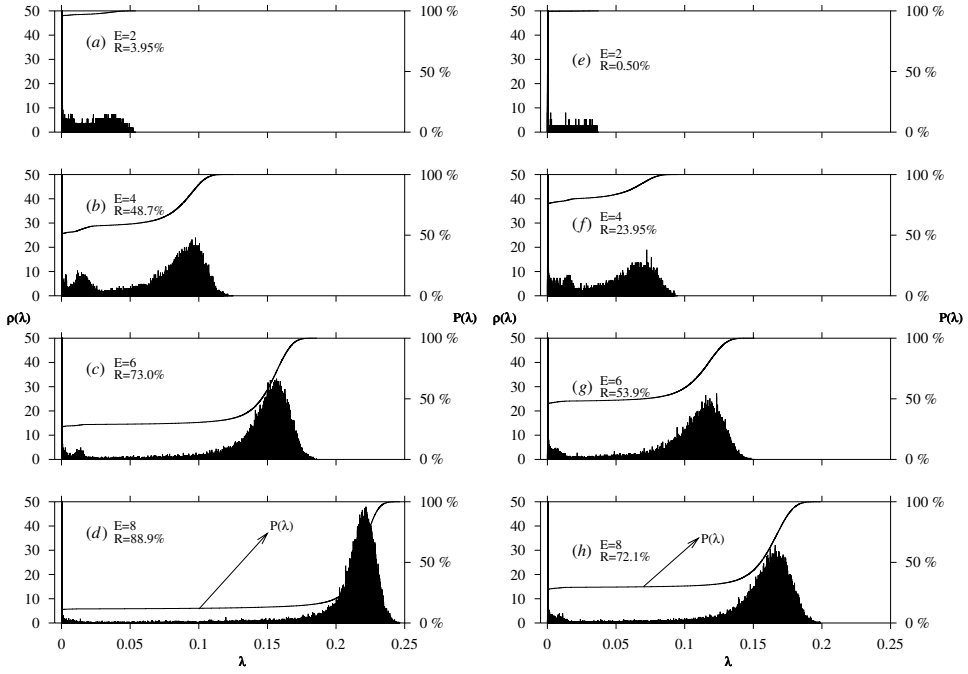

Figure 7. Distribution of positive Lyapunov exponents. Classical system (left column) and quantum system (right column). $v_{22} = 0.25$.

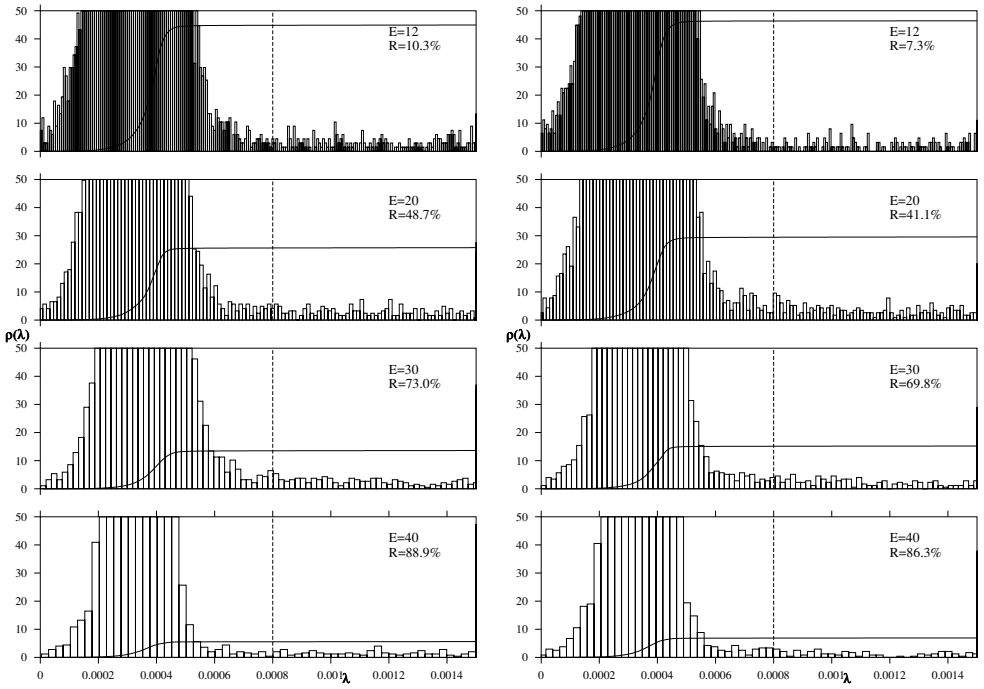

Figure 8. Distribution of Lyapunov exponents near $\lambda = 0$ for different energies E. Classical system (left column) and quantum system (right column). $v_{22} = 0.05$.

the degree of chaoticity in the classical system, has a counterpart in the parameter $\tilde{v}_{22}$ in the quantum system, which plays a similar role. For all energies, and all values of v_{22}, R plotted in figure 10 is smaller in the quantum system than in the corresponding classical system, i.e. the classical system turns out to be more chaotic than the quantum system. This is the main result of this work.

How can we understand the observed behaviour? The distribution of Lyapunov exponents approaching a Gaussian with increasing energy is well known from Hamiltonian systems with mixed dynamics [27]. The shape of the curve and its decreasing width can be understood as a consequence of the central limit theorem, which predicts such behaviour for an arithmetic mean of N random variables for $N \to \infty$. On the other hand, regular islands in an otherwise chaotic phase space are known to give non-Gaussian tails. What can we say about those tails? In Hamiltonian chaotic systems, with increasing energy, the phase space becomes more chaotic, i.e. regular islands become smaller or disappear. Thus it is plausible that the non-Gaussian tails of the distribution of positive Lyaponov exponents, associated with the regular islands, diminish. We have estimated numerically the weight of non-Gaussian tails using a fit of the data by a Gaussian distribution. For example, in the distribution of classical Lyapunov exponents corresponding to $v_{22} = 0.25$ (see the left column of figure 7), the relative error ϵ of such fits is as follows: $E = 2, \epsilon = 0.60, E = 4, \epsilon = 0.39$, $E = 6, \epsilon = 0.30, E = 8, \epsilon = 0.27$, which diminishes with increasing energy. Qualitatively similar behaviour is found in the corresponding quantum Lyapunov exponents as well as for the data corresponding to the coupling parameter $v_{22} = 0.05$.

Second, quantum fluctuations which occur in the parameters of the quantum action can be viewed as renormalization effects of the classical parameters [19]. The value of v_2 (if sole term

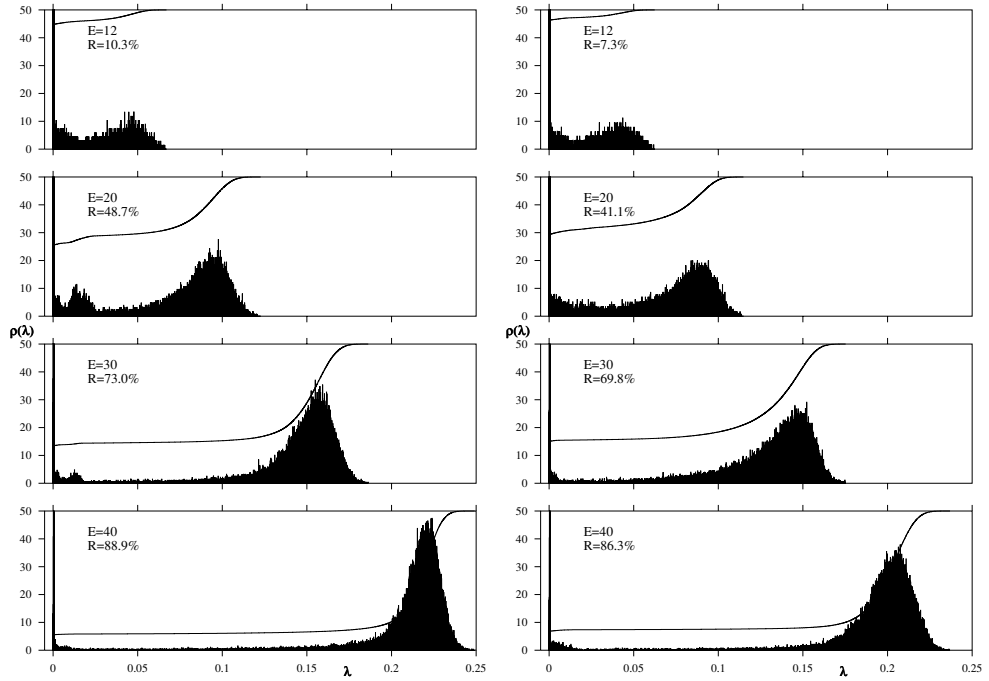

Figure 9. Distribution of positive Lyapunov exponents. Classical system (left column) and quantum system (right column). $v_{22} = 0.05$.

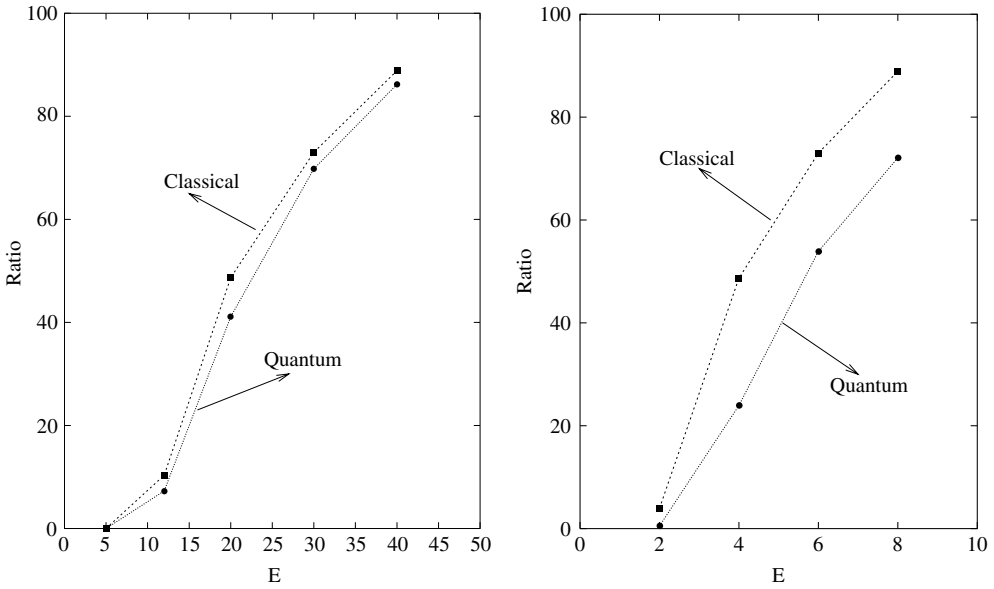

Figure 10. Volume of chaotic phase space (positive Lyapunov exponent) over total phase space (lines are guides to the eye). Left $v_{22} = 0.05$, right $v_{22} = 0.25$.

of potential would render the system integrable) is increased, while v_{22} (term which drives the system away from integrability) is decreased (see table 1). Hence chaos is reduced in the quantum system. Such increase of the quadratic term has been observed in other systems also and seems to occur more generally.

5. Conclusion

What is the significance of our findings? In particular, what is the physical significance of chaotic properties of trajectories for the quantum system?

(i) We found that the quantum action for large transition times allows us to construct a quantum analogue phase space for Hamiltonian systems with mixed chaotic dynamics. Such phase space resembles the classical phase space, in particular, when the parameter driving chaos is small. For the mixed system considered, the quantum analogue phase space, like classical phase space, shows islands of regular behaviour interwoven with chaotic regions. Moreover, hyperbolic fixed points occurring in the classical phase space survive in the quantum phase space. We compared quantitatively the classical system with the quantum system and found that the latter is systematically less chaotic than the former. The reason for such behaviour, in our opinion, is the tendency of quantum fluctuations to drive the quantum action nearer to a Gaussian fixed point. Moreover, we have investigated the quantum analogue phase space as a function of energy. We find that such phase space, like the classical phase space, becomes more chaotic when energy increases. Thus introducing a quantum analogue phase space gives a detailed and quantitative measure reflecting how much chaos grows as a function of energy.

(ii) The significance of trajectories can be seen by drawing an analogy with the interpretation of scattering experiments. In a scattering experiment, one usually measures counting rates in detectors, which when positioned at different angles give a differential cross section. Using theoretical input, like the S-matrix, unitarity and symmetries such as rotational symmetry of the potential, one can obtain derived quantities, such as scattering phase shifts $\delta_l(E)$. They give a picture of scattering as a function of energy and indicate the existence of resonances in certain channels (jumps of phase shift). The partial wave expansion in conjunction with phase shifts $\delta_l(E)$ gives a representation of the S-matrix and of scattering cross sections. In analogy with this picture, we consider the quantum action and its trajectories as a parametrization of the quantum mechanical transition amplitudes. The quantum action and its trajectories are derived quantities. These trajectories in conjunction with tools of nonlinear dynamics (Poincaré sections, Lyapunov exponents) give a picture of (make 'visible') the chaotic dynamics in the quantum system. One may view the Lyapunov exponents computed from trajectories of the quantum action in analogy with scattering phase shifts computed from a partial wave analysis of scattering cross sections.

(iii) The trajectories of the quantum analogue phase space gain a particular importance in the interpretation of the phenomenon of chaos assisted quantum dynamical tunnelling. This phenomenon is similar to tunnelling through a potential barrier; however, in this case the classical transition is forbidden by a dynamical law, the presence of a KAM surface. The experiments with ultracold atoms in an amplitude modulated optical standing wave reported by Hensinger *et al* [28] and Steck *et al* [29] demonstrate that such dynamical tunnelling exists and its amplitude is enhanced by chaos. The tunnelling occurs between regions which in classical phase space correspond to regions of stable motion (fixed points). In the quantum system this region is associated with eigenstates of the Floquet

operator. Hensinger *et al* point out that 'Floquet states do not necessarily overlap well with the regions of regular motion of the classical Poincaré map, except in the semi-classical limit'. Steck *et al* work with wave packets narrow in momentum space but not localized in position. In order to get a picture of phase space they use a classical phase space with a distribution with the same position and momentum marginal distribution as the Wigner function. We suggest that in order to better understand the mechanism of dynamical tunnelling, the role of localized states, decoherence, a higher number of Floquet states, a quantum analogue phase space and its trajectories from the quantum action are a complementary tool and should give additional useful insight into the dynamics of the quantum system.

Acknowledgments

HK and KM are grateful for support by NSERC Canada. GM and DH have been supported by FCAR Québec. For discussions and constructive suggestions HK is very grateful to A Okopinska and B Eckhardt.

References

[1] Friedrich H and Wintgen D 1989 *Phys. Rep.* **183** 37
[2] Bohigas O, Tomsovic S and Ullmo D 1993 *Phys. Rep.* **223** 43
[3] Percival I C 1973 *J. Phys. B: At. Mol. Phys.* **6** L229–32
[4] Brody T A, Flores J, French J B, Mello P A, Pandey A and Wong S S M 1981 *Rev. Mod. Phys.* **53** 385
[5] Izrailev F M 1990 *Phys. Rep.* **196** 299
[6] Lenz G and Haake F 1991 *Phys. Rev. Lett.* **67** 1
[7] Berry M V and Robnik M 1984 *J. Phys. A: Math. Gen.* **17** 2413
[8] Cametti F, Jona-Lasinio G, Presilla C and Toninelli F 2000 *Proc. Int. School of Phys. Enrico Fermi* ed G Casati *et al* (Amsterdam: IOS Press) p 431 (*Preprint* quant-ph/9910065)
[9] Schwengelbeck U and Faisal F H M 1995 *Phys. Lett.* A **199** 281
[10] Parmenter R H and Valentine R W 1995 *Phys. Lett.* A **201** 1
[11] Iacomelli G and Pettini M 1996 *Phys. Lett.* A **212** 29
[12] Partovi M H 2002 *Phys. Rev. Lett.* **89** 144101
[13] Casetti L, Gatto R and Modugno M 1998 *Phys. Rev.* E **57** 1223
[14] Matinyan S G and Müller B 1997 *Phys. Rev. Lett.* **78** 2515
[15] Jirari H, Kröger H, Luo X Q, Moriarty K J M and Rubin S G 2001 *Phys. Rev. Lett.* **86** 187
[16] Jirari H, Kröger H, Luo X Q, Moriarty K J M and Rubin S G 2001 *Phys. Lett.* A **281** 1
[17] Caron L A, Jirari H, Kröger H, Luo X Q, Melkonyan G and Moriarty K J M 2001 *Phys. Lett.* A **288** 145
[18] Kröger H 2002 *Phys. Rev.* A **65** 052118 (see equation (37))
[19] Jirari H, Kröger H, Luo X Q, Melkonyan G and Moriarty K J M 2002 *Phys. Lett.* A **303** 299
[20] Huard D, Kröger H, Melkonyan G, Moriarty K J M and Nadeau L P 2003 *Phys. Rev.* A **68** 034101
[21] Witten E 1981 *Nucl. Phys.* B **185** 513
[22] Bernstein M and Brown L S 1984 *Phys. Rev. Lett.* **52** 1933
[23] Kumar P, Ruiz-Altaba M and Thomas B S 1986 *Phys. Rev. Lett.* **57** 2749
[24] Keung W Y, Kovacs E and Sukhatme U P 1988 *Phys. Rev. Lett.* **60** 41
[25] Dahlqvist P and Russberg G 1990 *Phys. Rev. Lett.* **65** 2837
[26] Pullen R A and Edmonds A R 1981 *J. Phys. A: Math. Gen.* **14** L477
[27] Prasad A and Ramaswamy R 1999 *Phys. Rev.* E **60** 2761
[28] Hensinger W K *et al* 2001 *Nature* **412** 52
[29] Steck D A, Oskay W H and Raizen M G 2001 *Science* **293** 274